Solid-State and Solution Structures of a Series of [(HBPz$_3^{Me2}$)Rh(CO)(PR$_3$)] and [(HBPz$_3^{Me2,4Cl}$)Rh(CO)(PR$_3$)] Complexes

François Malbosc,[a] Valérie Chauby,[a] Carole Serra-Le Berre,[a] Michel Etienne,[b] Jean-Claude Daran,[b] and Philippe Kalck*[a]

Keywords: Pyrazolylborato ligands / Rhodium / IR spectroscopy / Square-planar complexes / Fluxional behavior

Addition of 1 equiv. of a phosphane or phosphite ligand to the κ^3-bonded [Tp^{Me2}Rh(CO)$_2$] and [Tp^{Me2,4Cl}Rh(CO)$_2$] dicarbonyl precursors gives the monosubstituted complexes [TpRh(CO)L]. The X-ray crystal structures show that the three complexes [Tp^{Me2}Rh(CO)(PMe$_3$)], [Tp^{Me2}Rh(CO)(PMePh$_2$)], and [Tp^{Me2,4Cl}Rh(CO)(PMePh$_2$)] adopt square-planar geometries. The X-ray crystal structure of [Tp^{Me2}Rh(CO){P(OPh)$_3$}] is consistent with an interaction between the dangling pyrazolyl group and the rhodium centre, the Rh–N distance being 2.762(3) Å. Analysis of ν(BH) and ν(CO) stretching frequencies shows that all the phosphane-containing complexes are square planar in solution as well as in the solid state. According to infrared analyses, the phosphite complexes [Tp^{Me2,4Cl}Rh(CO){P(OPh)$_3$}] and [Tp^{Me2,4Cl}Rh(CO){P(OMe)$_3$}] adopt a pentacoordinated geometry both in the solid state and in solution. However, the infrared data for [Tp^{Me2}Rh(CO){P(OPh)$_3$}] and [Tp^{Me2}Rh(CO){P(OMe)$_3$}] indicate that the Tp^{Me2} ligand is in a κ^3 coordination mode in the solid state, as already evidenced by the X-ray crystal structure, but in a κ^2 mode in solution. We also describe an exchange phenomenon between dangling and coordinated pyrazolyl groups, as studied by NMR.

Introduction

Since the first report of pyrazolylborato ligands by Trofimenko in 1966,[1] hydrotris(pyrazolyl)borates have been extensively used as σ donor ligands in a wide variety of transition metal complexes.[2] They can provide stable complexes, e.g. by replacing the isoelectronic cyclopentadienyl and pentamethylcyclopentadienyl ligands, and offer greater flexibility. Indeed, these ligands can adopt various modes of coordination ranging from the ubiquitous κ^3 and κ^2 forms to the less common κ^1 coordination mode.[3,4] Even rarer is their recently recognized ability to act as counterions (i.e., a κ^0 form)[5] in transition metal salts. Venanzi and co-workers have studied the geometry adopted in solution by complexes of the type [{HB(3R,4R′,5R"-pyrazolyl)$_3$}Ir(η^4-C$_8$H$_{12}$)], or, using the nomenclature of Trofimenko,[2] of the type [Tp$^{3R,4R',5R''}$Ir(COD)].[6] In its κ^2 coordination mode, the ligand can have the non-coordinated pyrazolyl group either far from the iridium centre or dangling in such a position that the κ^3 mode can readily be achieved, as depicted in Scheme 1.

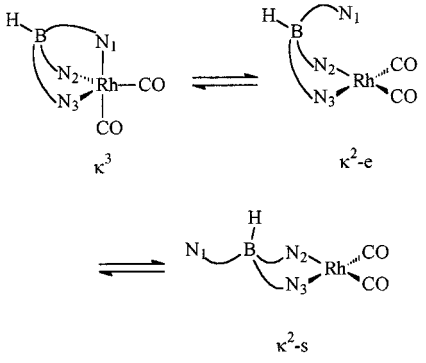

Scheme 1. The three coordination modes of Tp (adapted from ref.[3])

Electronic and steric effects of each pyrazolyl group play an important role in determining the equilibrium between the three different forms κ^2-e (the pyrazolyl in a pseudo-equatorial position), κ^2-s (scorpionate[6]), and κ^3. The nature of the substituent in the 3-position, i.e. adjacent to the potentially coordinating nitrogen atom, exerts a strong influence on this equilibrium. More specifically, steric hindrance between an R substituent in the 3-position and the hydrogen atoms of the two double bonds of the cyclooctadiene ligand in [Tp$^{3R,4R',5R''}$Ir(C$_8$H$_{12}$)] plays an important role.[6] Venanzi and co-workers,[6] as well as Akita, Moro-oka et al. for related [Tp^{iPr}Rh(diene)] complexes,[7] have used the wavenumber of the ν(BH) stretching vibration to assign a κ^2 or a κ^3 bonding mode for the Tp ligand. When ν(BH) is near to 2470 cm^{-1}, a square-planar complex in a κ^2 mode is observed, whereas a ν(BH) band at around 2540 cm^{-1} is indicative of a trigonal-bipyramidal structure with a κ^3 coordination mode.[7]

This class of complexes has become of particular interest since Ghosh and Graham demonstrated that [Tp^{Me2}Rh(CO)$_2$] photochemically activates one C–H bond of benzene or cyclohexane to afford the corresponding hydrido phenyl or cyclohexyl rhodium complexes.[8] This latter complex reacts with methane to afford

[a] Laboratoire de Catalyse, Chimie Fine et Polymères, ENSCT, 118 route de Narbonne, 31077 Toulouse Cedex, France
[b] Laboratoire de Chimie de Coordination du CNRS, 205 route de Narbonne, 31062 Toulouse Cedex, France

 © WILEY-VCH Verlag GmbH, 69451 Weinheim, 2001 1434–1948/01/1010–2689 $ 17.50+.50/0

[Tp^{Me2}Rh(CO)(H)(CH_3)]. The mechanism of this photochemically induced C−H bond activation has been studied by Purwoko and Lees,[9] as well as by Bergman and coworkers.[10] The process is believed to involve a sequence of elimination of a CO ligand, coordination of the C−H bond in an η^2 mode, a change from κ^3 to κ^2 bonding of the Tp^{Me2} ligand to the rhodium, and finally oxidative addition of the alkane.[7] The observation of the intermediate [(κ^2-Tp^{Me2})Rh(CO)(η^2-RH)] has prompted us to report the preparation of a series of [Tp′Rh(CO)(PR_3)] complexes, which were designed to have a more nucleophilic centre with a view to enhancing their C−H activating ability. The present paper deals with the preparation and characterization of [Tp^{Me2}Rh(CO)L] and [$Tp^{Me2,4Cl}$Rh(CO)L] (L = phosphane, phosphite) complexes. We have performed a detailed study of their solid-state and solution structures, as probed by infrared and NMR spectroscopies, and by X-ray crystal structure determinations. While this project was in progress,[11] the synthesis of [Tp^{Me2}Rh(CO)(PPh_3)] was published.[12] Several [Tp^{Me2}Rh(CO)(PR_3)] complexes have been described in the Ph.D. thesis of C. K. Ghosh.[13]

Results and Discussion

Preparation of [Tp^{Me2}Rh(CO)(PR_3)] and [$Tp^{Me2,4Cl}$Rh(CO)(PR_3)] Complexes

Addition of one equivalent of a phosphane or a phosphite ligand PR_3 to [Tp^{Me2}Rh(CO)$_2$] (**1**) or [$Tp^{Me2,4Cl}$Rh(CO)$_2$] (**2**) at room temperature results in the substitution of one CO ligand to afford the corresponding [TpRh(CO)(PR_3)] complexes as shown in Equations (1) and (2).

$$[Tp^{Me2}Rh(CO)_2] + PR_3 \longrightarrow [Tp^{Me2}Rh(CO)(PR_3)] + CO \quad (1)$$

1

PR_3 = PMe_3: **3**; PMe_2Ph: **4**; $PMePh_2$: **5**; PPh_3: **6**; $P(OMe)_3$: **7**; $P(OPh)_3$: **8**

$$[Tp^{Me2,4Cl}Rh(CO)_2] + PR_3 \longrightarrow [Tp^{Me2,4Cl}Rh(CO)(PR_3)] + CO \quad (2)$$

2

PR_3 = PCy_3: **9**; PMe_3: **10**; PMe_2Ph: **11**; $PMePh_2$: **12**; PPh_3: **13**; $P(OMe)_3$: **14**; $P(OPh)_3$: **15**; $P(OiPr)_3$: **16**

The rate of this reaction is determined by the nature of the ligand. The more basic but sterically hindered tricyclohexylphosphane PCy_3 reacts with **2** within about 1 h to give **9**. The ligands PMe_3, PMe_2Ph, $PMePh_2$, and even $P(OMe)_3$ react within a few minutes, as monitored by infrared spectroscopy. The syntheses of **8**, **15**, and **16**, containing the less basic ligands $P(OPh)_3$ and $P(OiPr)_3$, require several hours. According to infrared data, these substitution reactions are quantitative and isolated yields are high (> 85%). In the case of complex **11**, PMe_2Ph in dichloromethane has to be added slowly at room temperature to avoid formation of the disubstituted complex [κ^1-$Tp^{Me2,4Cl}$Rh(CO)(PMe_2Ph)$_2$].[4] **11** can then be recrystallized at low temperature, leaving **2** and the bis-adduct in solution. All the complexes have been fully characterized by infrared, ^{1}H, and ^{31}P NMR, and in some cases by ^{13}C and ^{103}Rh NMR. The solid-state structures of **3**, **5**, **8**, and **12** have been confirmed by X-ray analyses.

Molecular Structures of the Complexes 3, 5, 8, and 12

X-ray crystal structures have been obtained for four complexes, two of which (**3** and **12**) have been described in brief in previous reports.[4,11] Salient data are presented in Table 1.

Table 1. Salient distances [Å] and angles [°] (SP = square plane) in complexes with PR_3: **3**, **5**, **8**, and **12**

	PMe_3: **3**	$P(OPh)_3$: **8**	$PMePh_2$: **5**	$PMePh_2$: **12**
Rh−C1	1.797(4)	1.802(4)	1.818(4)	1.810(2)
Rh−P1	2.2447(9)	2.1794(9)	2.2503(9)	2.258(5)
Rh−N1	2.113(3)	2.110(3)	2.097(3)	2.0923(15)
Rh−N3	2.101(3)	2.097(3)	2.095(3)	2.0911(16)
Rh−N5	3.632(3)	2.762(3)	3.661(4)	3.800(2)
Pz_3−SP angle	55.05	78.91	52.12	48.05
N6−B1−H1	109.9	111.7(20)	115.5(22)	113.3(14)

We first focus on the structures of **5** and **12**, which have the same $PMePh_2$ phosphane ligand. Both complexes show the same square-planar environment (see Figure 1 for **5** and Figure 2 for **12**), with two pyrazolyl groups bonded to the rhodium metal centre and the third one in a dangling position. The Rh−N5 distances of 3.661(4) and 3.800(2) Å in **5** and **12**, respectively, preclude any bonding interaction between these atoms. The difference between these distances is due to the rotation of the free pyrazolyl group, since the angle between the pyrazolyl and the square plane varies from 52.12° to 48.05°. The Rh−N1, Rh−N3, and Rh−P1 distances can be considered as being the same in these complexes. Within each complex, the Rh−N distances to the coordinated pyrazolyl groups, Rh−N1 and Rh−N3, are equal, irrespective of the ligand in the *trans* position (i.e. CO or $PMePh_2$). As usual, the ν(CO) stretching frequencies are more sensitive to the electronic modifications of the metal centre than the Rh−C, C−O, and Rh−O distances for the CO ligands. Indeed, the four Rh−O1 bond lengths for **3**, **5**, **8**, and **12** are 2.949 [ν(CO) = 1961 cm^{-1}], 2.954 (1984 cm^{-1}), 3.099 (1975 cm^{-1}), and 2.910 Å (1996 cm^{-1}), respectively. A square-planar environment is also found for **3** (Figure 3), and the Rh−N1 and Rh−N3 bond lengths are identical within experimental error.

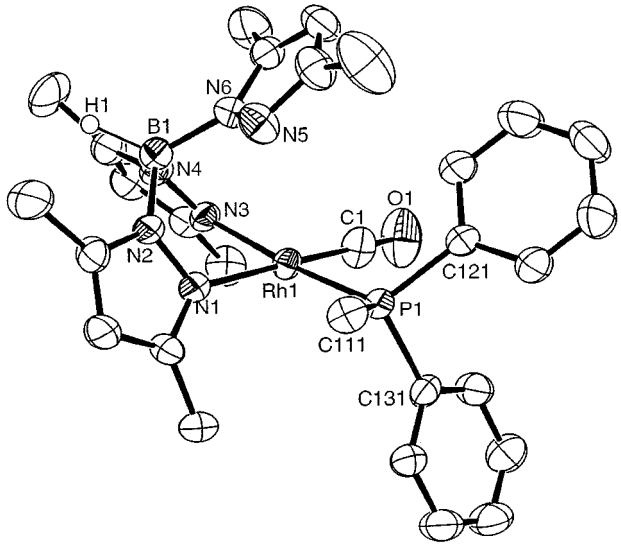

Figure 1. Molecular view of complex **5**; ellipsoids are drawn at a 30% probability level

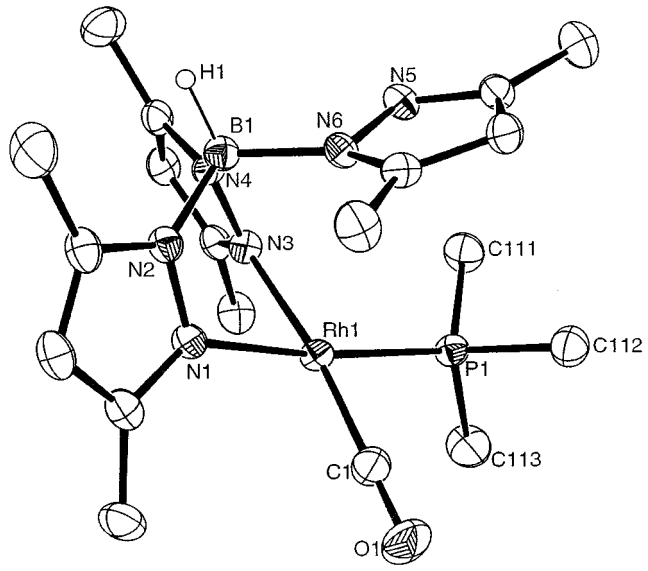

Figure 3. Molecular view of complex **3**; ellipsoids are drawn at a 30% probability level

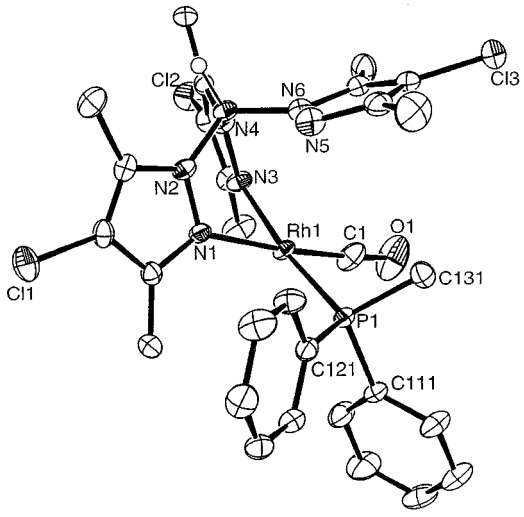

Figure 2. Molecular view of complex **12**; ellipsoids are drawn at a 30% probability level

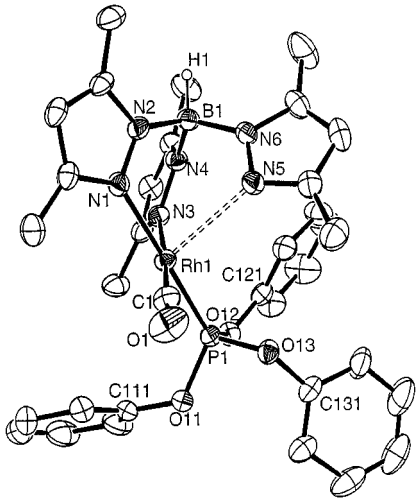

Figure 4. Molecular view of complex **8**; ellipsoids are drawn at a 30% probability level

Complex [Tp^{Me2}Rh(CO){P(OPh)$_3$}], **8**, has also been analysed by X-ray crystallography, in view of its unexpected infrared spectra (vide infra). The geometry about the rhodium is again square-planar (Figure 4). The most notable feature is an Rh−P1 distance of 2.1794(9) Å, which is significantly shorter than the Rh−P1 distances observed with PMe_3 in **3** (2.245 Å) or with $PMePh_2$ in **5** and **12** (2.250 Å and 2.258 Å, respectively). This is consistent with the better π-accepting properties of a phosphite as compared to a phosphane. A further feature deserves comment. The Rh−N5 distance is 2.762(3) Å, longer than that of a true coordination bond (ca. 2.1 Å), but shorter than the sum of the van der Waals radii (3.3 Å). Such a distance is thus consistent with an Rh−N5 interaction. Recently, Connelly et al. reported the X-ray structure of [Tp^{Me2}Rh(CO)(PPh$_3$)], which has a square-planar geometry with Tp^{Me2} adopting a κ^2 coordination mode.[12] One-electron oxidation results in the formation of [Tp^{Me2}Rh(CO)(PPh$_3$)]$^+$, X-ray analysis of which showed it to contain a κ^3-Tp^{Me2}. The rhodium(II) centre is then in a square-pyramidal environment, with the axial Rh−N5 bond length being 2.224(2) Å as opposed to 2.091(2) Å and 2.093(2) Å for the two other rhodium−nitrogen distances. Thus, the P(OPh)$_3$-containing complex **8** shows a lengthening of ca. 0.5 Å when compared to the rhodium(II) complex. Overall, we conclude that a κ^3 coordination mode is favoured by a decrease in the electron density at the metal centre.

Infrared Study of Complexes 3−15

Previous studies have shown that the ν(BH) stretching frequency offers a reliable means of ascertaining the coordination mode of tris(pyrazolyl)borato ligands.[6,7] Particularly

interesting are the absolute values of the ν(BH) frequencies determined by Moro-oka et al., which are ca. 2470 cm^{-1} for κ^2 coordination and 2540 cm^{-1} for κ^3 coordination.[7] The measured ν(BH) values for all the complexes are presented in Tables 2 and 3. Spectra were obtained from samples in both KBr and CH_2Cl_2. For the complexes bearing more basic phosphanes, i.e. those with PR_3 = PMe_3, PMe_2Ph, $PMePh_2$, and PPh_3 (**3−6** and **9−13**), the ν(BH) values are near to 2480 cm^{-1} and 2485 cm^{-1} in the solid state and in solution, respectively, irrespective of the Tp′ ligand. Figure 5 shows a plot of ν(BH) in CH_2Cl_2 as a function of the basicity of the phosphorus ligand on the Derencsényi scale;[14] ν(BH) is seen to be independent of the phosphane basicity, i.e. it is only weakly sensitive to the electron density at the metal centre. Thus, complexes **3−6** and **9−13** consistently show square-planar geometries, with Tp^{Me2} and $Tp^{Me2,4Cl}$ adopting the κ^2 coordination mode. The diagnostic criterion of Moro-oka et al., as established for [Tp^{Me2}Rh(diene)], is also valid here.

Table 2. ν(BH) and ν(CO) stretching frequencies for the complexes [Tp^{Me2}Rh(CO)(PR_3)] in KBr dispersions and in CH_2Cl_2 solutions

[Tp^{Me2}Rh(CO)(PR_3)]	ν(BH) [cm^{-1}] CH_2Cl_2	KBr	ν(CO) [cm^{-1}] CH_2Cl_2	KBr
$P(OPh)_3$	2479	2518	2009	1984
$P(OMe)_3$	2477	2508	1996	1963
PPh_3	2472	2468	1978	1965
$PMePh_2$	2476	2463	1979	1975
PMe_2Ph	2473	2464	1973	1968
PMe_3	2470	2443	1969	1961

Table 3. ν(BH) and ν(CO) stretching frequencies for the complexes [$Tp^{Me2,4Cl}$Rh(CO)(PR_3)] in KBr dispersions and in CH_2Cl_2 solutions

[$Tp^{Me2,4Cl}$Rh(CO)(PR_3)]	ν(BH) [cm^{-1}] CH_2Cl_2	KBr	ν(CO) [cm^{-1}] CH_2Cl_2	KBr
$P(OPh)_3$	2554	2542	2010	2004
$P(OiPr)_3$	2483	2469	1995	1996
$P(OMe)_3$	2553	2536	2002	1998
PPh_3	2482	2477	1984	1988
$PMePh_2$	2486	2477	1985	1996
PMe_2Ph	2485	2482	1981	1978
PMe_3	2484	2477	1973	1963
PCy_3	2483	2483	1973	1977

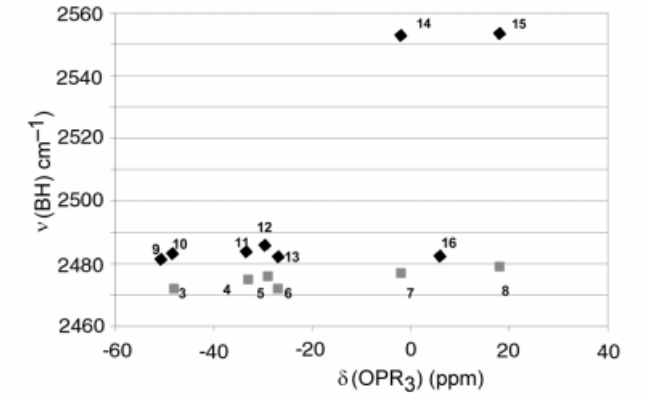

Figure 5. The ν(BH) values for complexes **3−16** in CH_2Cl_2 solution plotted as a function of phosphane basicity on the Derencsényi scale

The situation is slightly more subtle when the less basic phosphite ligands are considered. For complexes **14** and **15**, the ν(BH) values (Table 3 and Figure 5) suggest that the coordination mode of the $Tp^{Me2,4Cl}$ ligand is κ^3. Hence, although we have been unable to obtain X-ray quality crystals to confirm the proposal, complexes **14** and **15** would seem to exhibit a pentacoordinated geometry. Interestingly, for the Tp^{Me2}-based complexes **7** and **8**, which contain the same $P(OMe)_3$ and $P(OPh)_3$ phosphite ligands, the ν(BH) frequencies are only consistent with a κ^2 coordination mode in CH_2Cl_2 solution (2477 and 2479 cm^{-1}, respectively). In contrast, data obtained in KBr suggest that a κ^3 mode is preferred in the solid state (2508 and 2518 cm^{-1} for **7** and **8**, respectively). This is reminiscent of the weaker interaction between the third pyrazolyl group and the rhodium centre revealed by the X-ray crystal structure of **8** (vide supra). Consequently, the Tp^{Me2} ligand is not in a genuine κ^3 coordination mode in **8**, but the position of the third pyrazolyl substituent induces a geometry around the boron atom that results in a ν(BH) band at around 2510 cm^{-1}.

As a further representative of the phosphite family in the [$Tp^{Me2,4Cl}$Rh(CO)(PR_3)] complexes, we have introduced $P(OiPr)_3$, the basicity of which is intermediate between those of $P(OMe)_3$ and PPh_3. Table 3 and Figure 5 unambiguously show that the environment in complex **16** is square-planar, from which we conclude that the steric hindrance induced by the phosphite ligand is sufficiently strong to compensate the decrease in electron density at the metal centre that would favour the approach of the third pyrazolyl group.

The ν(CO) stretching frequencies were measured both in solution and in the solid state for all the complexes (Tables 2 and 3). Figure 6 shows a plot of ν(CO) as a function of the basicity of the PR_3 ligand (CH_2Cl_2 solution). The points representing those complexes having a κ^2-bonded Tp^{Me2} ligand lie on a straight line with a correlation coefficient of 0.98. As usual, the ν(CO) frequencies reliably reflect the electron density at Rh as the basicity of the ligand is varied.

For complexes **9−16**, the situation is less straightforward. A straight line can clearly be seen in Figure 6 for complexes **9−13** and **16**, which exhibit a κ^2 coordination mode in solution. This is in agreement with the conclusions drawn from the analysis of the ν(BH) frequencies. However, the ν(CO) values for complexes **14** and **15** lie at higher frequencies. The corresponding points in the plot do not fall on the previous straight line, but the line plotted between these two points is parallel to the first one. Thus, Figure 6 shows the monotonous variations in the electron density in [κ^2-$Tp^{Me2,4Cl}$Rh(CO)(PR_3)] (lower line) and [κ^3-$Tp^{Me2,4Cl}$Rh(CO){$P(OR)_3$}] (upper line). It is important to note that we might have expected a decrease in the ν(CO) stretching frequency due to the coordination of the third pyrazolyl group, i.e. a line in the plot lower than the κ^2

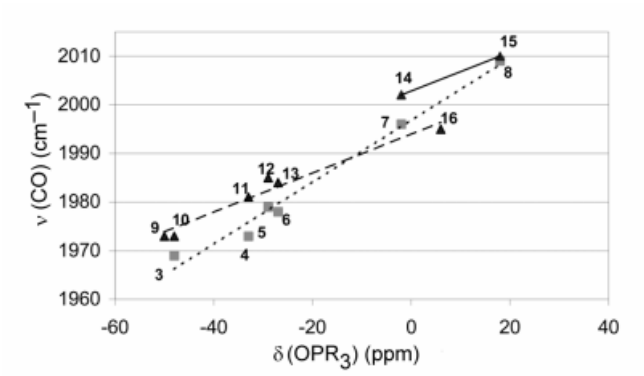

Figure 6. The ν(CO) frequencies for complexes **3**−**16** in CH_2Cl_2 solution plotted as a function of phosphane basicity on the Derencsényi scale

straight line. In fact, this coordination leads to a pentacoordinated geometry, in which the CO force constant is no longer comparable to that for a square-planar geometry.

NMR Studies; Fluxionality of Complexes 3−15

Most of the complexes have been studied by ^{1}H, ^{13}C, ^{31}P, and ^{103}Rh NMR, and in some cases at variable temperature as they are fluxional. We were particularly interested in the PMe_2Ph-containing complex **4** since, in its square-planar environment and with the third pyrazolyl group in a dangling position, as a result of which the plane of symmetry is lost, two diastereotopic methyl groups are to be expected. However, the ^{1}H NMR spectrum recorded at room temperature (Figure 7) features a doublet due to the Me groups of the PMe_2Ph ligand (J_{PH} = 9 Hz) and two singlets at δ = 2.15 and 2.21 due to the Tp^{Me2} methyl substituents. At 183 K (Figure 8), the signal due to the phosphane methyl protons is broader, two methyl groups of a pyrazolyl group give rise to signals at δ = 2.32 and 2.75, while the four remaining Tp^{Me2} methyls give rise to two signals at δ = 1.88 (broad) and 2.05. Thus, the NMR spectra show a non-rigidity for this complex, although the slow-exchange limit was not reached.

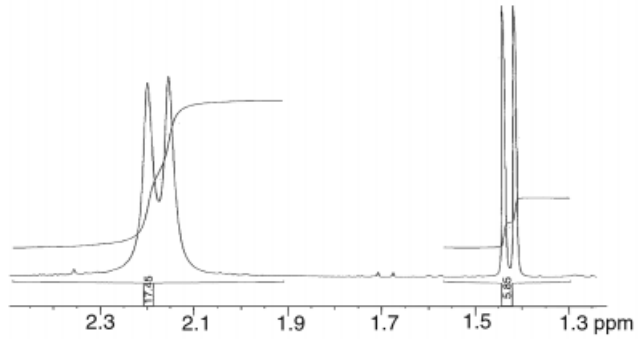

Figure 7. ^{1}H NMR spectrum of complex **4** at 293 K

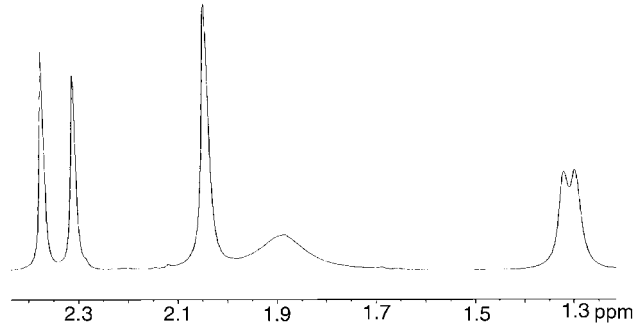

Figure 8. ^{1}H NMR spectrum of complex **4** at 183 K

In order to assign the signals in a situation in which the stereochemical non-rigidity of the complex would be avoided, we protonated **4** with 1 equiv. of HBF_4, a reaction yielding [{κ^2-HB(Pz^{Me2})$_2$(HPz^{Me2})}Rh(CO)(PMe$_2$Ph)][BF$_4$] (**4H$^+$**).[15] The infrared spectrum of **4H$^+$** in KBr shows ν(CO) and ν(BH) bands at 1987 and 2502 cm^{-1}, respectively, close to those of **4** (1968 and 2464 cm^{-1}). Direct protonation at the rhodium centre would have led to a shift in the position of the ν(CO) band of between 50 and 100 cm^{-1}. No ν(Rh−H) band was observed. These data are consistent with a square-planar environment for the rhodium atom and a κ^2 coordination mode for the Tp^{Me2} ligand. No spectroscopic evidence for a hydrido ligand was found, but a ^{1}H NMR signal at δ = 11.84 is consistent with the presence of an NH group. Thus, protonation of **4** occurs on the free pyrazolyl arm as expected. The methyl region of the ^{1}H NMR spectrum shown in Figure 9 confirms the absence of a symmetry plane in **4H$^+$**. The two methyls of PMe_2Ph are diastereotopic and six Tp^{Me2} methyl signals are observed. An Rh−H coupling (1.6 Hz) is apparent from the higher field doublet. With the aid of {^{1}H,^{1}H}, {^{1}H,^{13}C} HMQC, and HMBC measurements and {^{1}H,^{1}H} NOESY experiments, all the ^{1}H NMR signals have been assigned, as shown in Figure 10. It is worth noting that the two lower field methyl peaks at δ = 2.38 and 2.48 are attributable to the 3-Me and 5-Me groups of the pyrazolyl group *trans* to the CO ligand, respectively. Moreover, there is no exchange between the two pyrazolyl groups bonded to rhodium.

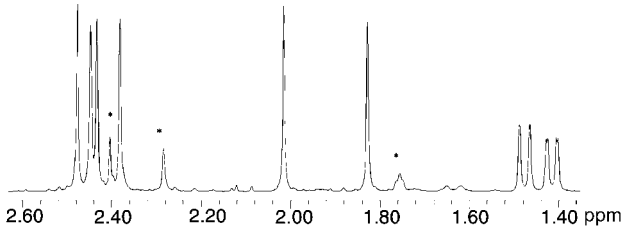

Figure 9. ^{1}H NMR spectrum of complex **4H$^+$**; *peaks attributable to the starting material **4**

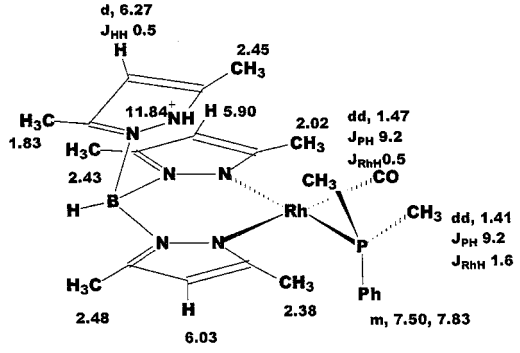

Figure 10. ^{1}H NMR signal assignments for complex **4H$^+$**

Study of the Exchange Phenomenon in 4

For complex **4** at 183 K (Figure 8), the two methyl proton signals observed at δ = 2.32 and 2.75 are assigned to the pyrazolyl *trans* to the CO ligand, these chemical shifts being very close to those of the pyrazolyl ligand *trans* to CO in **4H**$^+$. Hence, the methyl signal at δ = 1.88 is attributable to the dangling pyrazolyl, while that at δ = 2.05 is due to the pyrazolyl *trans* to the phosphane. The exchange rate for the former is slightly higher than the rate corresponding to the coalescence temperature. At low temperature, the latter pyrazolyl methyl groups undergo exchange with a low activation energy. Since the pyrazolyl *trans* to CO is not involved in the exchange phenomenon, we propose a square-pyramidal transition state, as shown in Figure 11. In a trigonal-bipyramidal transition state, the apical pyrazolyl group would exchange at the same rate with either of the two equatorial groups. When the temperature is raised, the third pyrazolyl *trans* to CO is also exchanged, so that the fast-exchange limit is reached at room temperature.

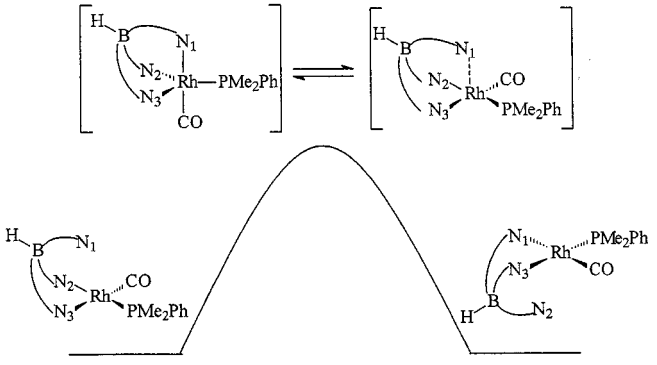

Figure 11. Proposed transition-state geometry for the exchange phenomenon between two square-planar isomers of **4**

This study shows that in a square-planar complex the pendant pyrazolyl group readily coordinates. Decoordination of the pyrazolyl *trans* to PMe_2Ph then provides the free pyrazolyl, as indicated in Figure 11. This phenomenon places the free pyrazolyl group either above or below the plane, such that the magnetic environments of the two methyl groups of PMe_2Ph become identical on the NMR time scale.[10]

The same exchange phenomenon has been observed for $[Tp^{Me2}Rh(CO)(PMe_3)]$,[11] $[Tp^{Me2,4Cl}Rh(CO)(PMePh_2)]$, and $[Tp^{Me2}Rh(CO)(PMePh_2)]$. For $[Tp^{Me2}Rh(CO)\{P(OPh)_3\}]$, however, the three pyrazolyl groups are still in fast exchange at 183 K. This is reminiscent of the results of the X-ray diffraction analysis, where the pendant pyrazolyl group and the rhodium centre were found to be in close proximity, and is consistent with the proposed geometry of the transition state and a low activation energy for the exchange between the square-planar isomers.

Conclusion

The complexes $[Tp^{Me2}Rh(CO)(PR_3)]$ and $[Tp^{Me2,4Cl}Rh(CO)(PR_3)]$ can readily be prepared by addition of one equivalent of the appropriate phosphane ligand to $[Tp^{Me2}Rh(CO)_2]$ and $[Tp^{Me2,4Cl}Rh(CO)_2]$, respectively. As shown by the X-ray crystal structures of four complexes and by an infrared study in the solid state and in solution, these complexes adopt a square-planar structure. In the case of a phosphite ligand, the dangling pyrazolyl group resides near the rhodium. The bonding mode is then intermediate between κ^2 and κ^3. NMR studies have shown a fluxional behaviour for all the $[Tp'Rh(CO)(PR_3)]$ complexes indicating that the more stable geometries are square-planar and that the transition state is close to square-pyramidal. Similar complexes have been prepared by Jones et al. with isocyanide ligands, while Carmona et al. have prepared iridium complexes with the general formula $[Tp'Ir(C_2H_4)(L)]$.[16,17]

Experimental Section

General Remarks: All experiments were carried out under argon. Reactions were performed using standard Schlenk techniques. Solvents were HPLC quality and were distilled under dinitrogen, toluene from sodium/benzophenone and dichloromethane from $CaSO_4$. They were frozen and degassed in vacuo, and were stored over molecular sieves under argon. Pentane was purified according to the method of Perrin and Armarego,[18] distilled from CaH_2 under argon, frozen, and degassed in vacuo. Commercial phosphites and phosphanes were used without purification. − NMR spectra were recorded with Bruker AC 200, WM 250, or AMX 400 spectrometers. − A Perkin−Elmer 1710 FT-IR spectrometer was used to record the infrared spectra. Solid samples were analysed in KBr and liquid samples were analysed between CaF_2 windows (vs: very strong, s: strong, m: medium, w: weak, vw: very weak, sh: shoulder). − X-ray analyses were performed with Enraf-Nonius CAD 4 or STOE IPDS diffractometers.

$HPz^{Me2,4Cl}$: This material[19] was prepared by the slow addition of hydrazine hydrate (20 mL, 412 mmol) to 3-chloro-2,4-pentanedione (49 mL, 411 mmol) in ethanol (600 mL) at 80 °C. The mixture was stirred for 3 h at 80 °C. After evaporation of the ethanol, the product was dissolved in CH_2Cl_2. The resulting solution was stirred with a small amount of $MgSO_4$ for 2 h and then filtered through Celite. The solvent was evaporated until crystallization commenced and then hexane (300 mL) was added. The solution was kept at 0 °C, whereupon white crystals were deposited. The crystals were washed with hexane (3 × 20 mL) at 0 °C and were then sublimed at 110 °C to yield 48.2 g (90%) of $HPz^{Me2,4Cl}$. − ^{1}H NMR ($CDCl_3$, 25 °C): δ = 2.24 (s, 6 H, CH_3). − IR (KBr): $\tilde{\nu}$ = 1588 cm^{-1} [ν(C=N)].

$KHBPz_3^{Me2,4Cl}$: This ligand[20] was prepared by the addition of 3,5-dimethyl-4-chloropyrazole (40.0 g, 307.2 mmol) to potassium tetrahydroborate (3.686 g, 68 mmol). The mixture was slowly heated to 120 °C. When the evolution of hydrogen had subsided, the temperature was raised to 220 °C. The reaction was seen to be complete when hydrogen evolution had ceased. Then, toluene (20 mL) was quickly added to avoid agglomeration of the product. The solution was concentrated to three-quarters of its original volume and then hexane (50 mL) was added. The resulting solution was kept at 0 °C. White crystals were deposited, which were washed with hexane (3 × 30 mL) at 0 °C. The crystals were freed of excess $HPz^{Me2,4Cl}$ by sublimation to yield 27.11 g (90%) of $KHBPz_3^{Me2,4Cl}$. − ^{1}H NMR ($CDCl_3$, 25 °C): δ = 2.00 [s, 9 H, $CH_3(Pz^{Me2,4Cl})$], 2.14 [s, 9

H, CH_3(Pz^{Me2,4Cl})]. − IR (KBr): $\tilde{\nu}$ = 2468 cm^{-1} [ν(BH)], 1541 cm^{-1} [ν(C=N)].

KHBPz$_3^{Me2}$: This ligand[21] was prepared by the addition of 3,5-dimethylpyrazole (15.0 g, 117.2 mmol) to potassium tetrahydroborate (1.405 g, 28 mmol). The mixture was slowly heated to 110 °C. When the evolution of hydrogen had subsided, the temperature was increased to 190 °C. The reaction was seen to be complete when the hydrogen evolution had ceased. Then, toluene (20 mL) was quickly added to avoid agglomeration of the product. The solution was concentrated to three-quarters of its original volume and then hexane (50 mL) was added. The resulting solution was kept at 0 °C. White crystals were deposited, which were washed with hexane (3 × 30 mL) at 0 °C. The crystals were freed of excess HPz^{Me2} by sublimation to yield 8.47 g (85%) of KHBPz$_3^{Me2}$. − ^{1}H NMR (CDCl$_3$, 25 °C): δ = 2.00 [s, 9 H, CH_3(Pz^{Me2})], 2.14 [s, 9 H, CH_3(Pz^{Me2})]. − IR (KBr): $\tilde{\nu}$ = 2438 cm^{-1} [ν(BH)], 1538 cm^{-1} [ν(C=N)].

[Rh(μ-Cl)(CO)$_2$]$_2$: This complex was prepared by bubbling CO through a solution of RhCl$_3$·3H$_2$O (3.0 g, 11.4 mmol) in methanol (100 mL) at 65 °C for 20 h. The methanol was then slowly evaporated by passing nitrogen through the solution. Red crystals were obtained, which were sublimed in vacuo at 50 °C to yield 4.21 g (95%) of the product. − IR (KBr): $\tilde{\nu}$ = 2102 m, 2082 s, 2020 s cm^{-1} [ν(CO)].

[Tp^{Me2}Rh(CO)$_2$] (1): Compound **1** was prepared by adding KHBPz$_3^{Me2}$ (1.89 g, 4.15 mmol) to a solution of [Rh(μ-Cl)(CO)$_2$]$_2$ (1.0 g, 2.57 mmol) in CH_2Cl_2 (60 mL). The mixture was stirred for 4 h, in the course of which it turned from yellow-orange to brown. The reaction was monitored by infrared spectroscopy. KCl formed during the reaction was filtered off and washed with CH_2Cl_2. The combined filtrate and washings were concentrated in vacuo, yielding 1.9 g (90%) of **1** as a yellow-orange solid. − ^{1}H NMR (C_6D_6, 25 °C): δ = 2.31, 2.37 [s, 6 H, CH_3(Pz^{Me2})], 5.77 [s, 3 H, CH(Pz^{Me2})]. − IR (KBr): $\tilde{\nu}$ = 2512 [ν(BH)], 2054 s, 1973 s cm^{-1} [ν(CO)]. − UV/Vis (pentane): λ_{max} = 355 nm.

[Tp^{Me2,4Cl}Rh(CO)$_2$] (2): Addition of solid KHBPz$_3^{Me2,4Cl}$ (2.26 g, 5.15 mmol) to a yellow-orange solution of [Rh(μ-Cl)(CO)$_2$]$_2$ (1.00 g, 2.57 mmol) in CH_2Cl_2 (60 mL) yielded a brown slurry after 4 h. The progress of the reaction was monitored by IR. The solution was then filtered and the removed solid was washed with CH_2Cl_2. The combined filtrate and washings were concentrated in vacuo, yielding 1.3 g (90%) of **2** as a yellow-orange solid. − ^{1}H NMR (C_6D_6, 25 °C): δ = 2.12, 2.41 [s, 6 H, CH_3(Pz^{Me2,4Cl})]. − IR (KBr): $\tilde{\nu}$ = 2544 [ν(BH)], 2088 w, 2059 s, 2020 w, 1984 s cm^{-1} [ν(CO)]. − UV/Vis (pentane): λ_{max} = 361 nm.

[Tp^{Me2}Rh(CO)(PMe$_3$)] (3): Complex **3** was prepared by adding PMe$_3$ (0.96 mL, 0.96 mmol, 1 M in toluene) to a solution of [Tp^{Me2}Rh(CO)$_2$] (0.4 g, 0.88 mmol) in CH_2Cl_2 (20 mL). The reaction was immediate, as indicated by a ν(CO) band at 1969 cm^{-1} in the IR spectrum. The solvent was then evaporated and the residue was washed with hexane at 0 °C and dried in vacuo at 40 °C for 6 h to yield 0.36 g (85%) of **3**. − ^{1}H NMR (C_6D_6, 25 °C): δ = 0.91 (d, 9 H, PMe$_3$, $^2J_{P-H}$ = 3 Hz), 1.75 [s, 9 H, CH_3(Pz^{Me2})], 2.15 [s, 9 H, CH_3(Pz^{Me2})]. − ^{31}P NMR (C_6D_6, 25 °C): δ = 5.02 (d, 1 P, $^1J_{Rh-P}$ = 145 Hz). − IR (KBr): $\tilde{\nu}$ = 2443 [ν(BH)], 1961 cm^{-1} [ν(CO)].

[Tp^{Me2}Rh(CO)(PMe$_2$Ph)] (4): Complex **4** was prepared by adding PMe$_2$Ph (62.4 μL, 0.44 mmol) to a solution of [Tp^{Me2}Rh(CO)$_2$] (0.20 g, 0.44 mmol) in CH_2Cl_2 (15 mL). The reaction was immediate, as shown by a ν(CO) band at 1973 cm^{-1} in the IR spectrum. The solvent was evaporated and the product was washed at 45 °C for 6 h, yielding 0.21 g (80%) of **4**. − ^{1}H NMR (C_6D_6, 25 °C): δ = 1.43 (d, 6 H, PMe$_2$, $^2J_{P-H}$ = 9 Hz), 2.15 [s, 9 H, CH_3(Pz^{Me2})], 2.21 [s, 9 H, CH_3(Pz^{Me2})], 5.83 [s, 3 H, CH(pz)], 7.82 (m, 5 H, PPh). − ^{31}P NMR (C_6D_6, 25 °C): δ = 20.13 (d, 1 P, $^1J_{Rh-P}$ = 151 Hz). − IR (KBr): $\tilde{\nu}$ = 2464 [ν(BH)], 1968 cm^{-1} [ν(CO)]. − $C_{24}H_{33}BN_6OPRh$ (566.3): calcd. C 50.91, H 5.87, N 14.84; found C 50.31, H 5.96, N 14.62.

[Tp^{Me2}Rh(CO)(PMePh$_2$)] (5): Complex **5** was prepared by adding PMePh$_2$ (89.7 μL, 0.48 mmol) to a solution of [Tp^{Me2}Rh(CO)$_2$] (0.20 g, 0.44 mmol) in CH_2Cl_2 (20 mL). The reaction was complete within 15 min, as shown by IR [ν(CO) = 1979 cm^{-1}]. The solution was filtered and the filtrate was concentrated to dryness. Crystallization of the residue from toluene/heptane at −18 °C yielded 0.23 g (85%) of yellow crystals of **5**. − ^{1}H NMR (C_6D_6, 25 °C): δ = 1.60 (dd, 3 H, P*Me*Ph$_2$, $^2J_{P-H}$ = 10, $^3J_{Rh-H}$ = 1 Hz), 2.05 [s, 9 H, CH_3(Pz^{Me2})], 2.32 [s, 9 H, CH_3(Pz^{Me2})], 5.71 [s, 3 H, CH(Pz^{Me2})], 7.42 (m, 10 H, PPh$_2$). − ^{31}P NMR (C_6D_6, 25 °C): δ = 30.60 (d, 1 P, $^1J_{Rh-P}$ = 155 Hz). − IR (KBr): $\tilde{\nu}$ = 2463 [ν(BH)], 1975 cm^{-1} [ν(CO)]. − UV/Vis (pentane): λ_{max} = 357 nm. − $C_{29}H_{35}BN_6OPRh$ (628.3): calcd. C 55.44, H 5.61, N 13.37; found C 52.40, H 5.16, N 12.34.

[Tp^{Me2}Rh(CO)(PPh$_3$)] (6): Complex **6** was prepared by adding solid PPh$_3$ (0.16 g, 0.48 mmol) to a solution of [Tp^{Me2}Rh(CO)$_2$] (0.20 g, 0.44 mmol) in CH_2Cl_2 (15 mL). The reaction was monitored by IR and was seen to be complete after 2 h [ν(CO) = 1978 cm^{-1}]. The solution was then filtered and the filtrate was concentrated to dryness. Crystallization of the residue from toluene/heptane at −18 °C yielded 0.24 g (80%) of yellow crystals of **6**. − ^{1}H NMR (C_6D_6, 25 °C): δ = 1.75 [s, 9 H, CH_3(Pz^{Me2})], 2.15 [s, 9 H, CH_3(Pz^{Me2})], 5.70 [s, 3 H, CH(Pz^{Me2})], 7.3 (m, 15 H, PPh$_3$). − ^{31}P NMR (C_6D_6, 25 °C): δ = 42.86 (d, 1 P, $^1J_{Rh-P}$ = 161 Hz). − IR (KBr): $\tilde{\nu}$ = 2468 [ν(BH)], 1965 cm^{-1} [ν(CO)]. − $C_{34}H_{37}BN_6OPRh$ (690.4): calcd. C 59.15, H 5.40, N 12.17; found C 59.48, H 5.47, N 11.90.

[Tp^{Me2}Rh(CO){P(OMe)$_3$}] (7): Complex **7** was prepared by adding P(OMe)$_3$ (52 μL, 0.44 mmol) to a solution of [Tp^{Me2}Rh(CO)$_2$] (0.20 g, 0.44 mmol) in CH_2Cl_2 (15 mL). The reaction was immediate, as shown by IR [ν(CO) = 1996 cm^{-1}]. The solvent was evaporated and the residue was washed with hexane at 0 °C and dried in vacuo to yield 0.19 g (85%) of **7**. − ^{1}H NMR (C_6D_6, 25 °C): δ = 1.92 [s, 9 H, CH_3(OMe$_3$)], 1.75 [s, 9 H, CH_3(Pz^{Me2})], 2.15 [s, 9 H, CH_3(Pz^{Me2})]. − ^{31}P NMR (C_6D_6, 25 °C): δ = 142.8 (d, 1 P, $^1J_{Rh-P}$ = 266 Hz). − IR (KBr): $\tilde{\nu}$ = 2508 [ν(BH)], 1963 cm^{-1} [ν(CO)].

[Tp^{Me2}Rh(CO){P(OPh)$_3$}] (8): Complex **8** was prepared by adding P(OPh)$_3$ (253 μL, 0.96 mmol) to a solution of [Tp^{Me2}Rh(CO)$_2$] (0.40 g, 0.87 mmol) in CH_2Cl_2 (20 mL). The reaction was complete within 2 h, as shown by IR [ν(CO) = 2009 cm^{-1}]. The solvent was then evaporated and the residue was washed with hexane at 0 °C and dried in vacuo at 45 °C for 6 h to yield 0.21 g (80%) of **8**. − ^{1}H NMR (C_6D_6, 25 °C): δ = 2.23 [s, 9 H, CH_3(Pz^{Me2})], 2.28 [s, 9 H, CH_3(Pz^{Me2})], 5.70 [s, 3 H, CH(Pz^{Me2})], 7.20 [m, 15 H, P(OPh)$_3$]. − ^{31}P NMR (C_6D_6, 25 °C): δ = 126.40 (d, 1 P, $^1J_{Rh-P}$ = 279 Hz). − IR (KBr): $\tilde{\nu}$ = 2518 [ν(BH)], 1984 cm^{-1} [ν(CO)]. − $C_{34}H_{37}BN_6O_4PRh$ (738.4): calcd. C 55.91, H 5.05, N 10.05; found C 55.30, H 5.04, N 11.38.

[Tp^{Me2,4Cl}Rh(CO)(PCy$_3$)] (9): Complex **9** was prepared by adding solid PCy$_3$ (0.16 g, 0.58 mmol) to a solution of [Tp^{Me2,4Cl}Rh(CO)$_2$] (0.30 g, 0.54 mmol) in toluene (30 mL). The mixture was stirred for

4 h. The solvent was then evaporated in vacuo and the yellow residue was washed three times with hexane at 0 °C and dried in vacuo to yield 0.39 g of **9**. − ^{1}H NMR (C_6D_6, 25 °C): δ = 1.75 (m, 33 H, PCy_3), 2.15 [s, 9 H, $CH_3(Pz^{Me2,4Cl})$], 2.30 [s, 9 H, $CH_3(Pz^{Me2,4Cl})$]. − ^{31}P NMR (C_6D_6, 25 °C): δ = 47.70 (d, $^2J_{Rh-P}$ = 152 Hz). − IR (KBr): $\tilde{\nu}$ = 2477 [ν(BH)], 1963 cm^{-1} [ν(CO)]. − UV/Vis (pentane): λ_{max} = 350 nm.

[Tp^{Me2,4Cl}Rh(CO)(PMe$_3$)] (10): Complex **10** was prepared by adding PMe_3 (0.4 mmol, 0.4 mL of a 1 M solution in toluene) to a solution of [Tp^{Me2,4Cl}Rh(CO)$_2$] (0.20 g, 0.37 mmol) in pentane (30 mL). The orange solution immediately turned yellow. The pentane was evaporated in vacuo to leave 0.20 g of **10** as a yellow solid. − ^{1}H NMR (C_6D_6, 25 °C): δ = 0.87 (d, 9 H, PMe_3, $^2J_{P-H}$ = 3 Hz), 2.09 [s, 9 H, $CH_3(Pz^{Me2,4Cl})$], 2.21 [s, 9 H, $CH_3(Pz^{Me2,4Cl})$]. − ^{31}P NMR (C_6D_6, 25 °C): δ = −9.66 (d, $^1J_{P-H}$ = 116 Hz). − IR (KBr): $\tilde{\nu}$ = 2477 [ν(BH)], 1963 cm^{-1} [ν(CO)]. − UV/Vis (pentane): λ_{max} = 350 nm.

[Tp^{Me2,4Cl}Rh(CO)(PMePh$_2$)] (12): Complex **12** was prepared by adding $PMePh_2$ (74 μL, 0.40 mmol) to a solution of [Tp^{Me2,4Cl}Rh(CO)$_2$] (0.20 g, 0.36 mmol) in pentane (30 mL) at 0 °C. A yellow solid was immediately precipitated, which was collected by filtration and dried in vacuo to afford a yellow powder. This powder was washed three times with hexane at 0 °C and dried in vacuo yielding 0.25 g of **12**. − ^{1}H NMR (C_6D_6, 25 °C): δ = 1.56 (dd, 3 H, P*Me*Ph$_2$, $^2J_{P-H}$ = 9, $^3J_{Rh-H}$ = 1 Hz), 2.09 [s, 9 H, $CH_3(Pz^{Me2,4Cl})$], 2.12 [s, 9 H, $CH_3(Pz^{Me2,4Cl})$], 7.08 (m, 10 H, PMe*Ph*$_2$). − ^{31}P NMR (C_6D_6, 25 °C): δ = 27.38 (d, 1 P, $^1J_{Rh-P}$ = 157 Hz). − IR (KBr): $\tilde{\nu}$ = 2477 [ν(BH)], 1996 cm^{-1} [ν(CO)]. − UV/Vis (pentane): λ_{max} = 352 nm.

[Tp^{Me2,4Cl}Rh(CO)(PPh$_3$)] (13): Complex **13** was prepared by adding solid PPh_3 (0.95 g, 0.36 mmol) to a solution of [Tp^{Me2,4Cl}Rh(CO)$_2$] (0.20 g, 0.36 mmol) in toluene (25 mL). The reaction was complete within 2 h. The solvent was then evaporated in vacuo yielding 0.25 g of a yellow solid. − ^{1}H NMR (C_6D_6, 25 °C): δ = 1.75 [s, 9 H, $CH_3(Pz^{Me2,4Cl})$], 2.15 [s, 9 H, $CH_3(Pz^{Me2,4Cl})$], 7.3 (m, 15 H, PPh_3). − ^{31}P NMR (C_6D_6, 25 °C): δ = 42.86 (d, 1 P, $^1J_{Rh-P}$ = 161 Hz). − ^{13}C{^{1}H} NMR (C_6D_6, 25 °C): δ = 9.86, 11.81 [s, $CH_3(Pz^{Me2,4Cl})$], 107.52 [s, $CH(Pz^{Me2,4Cl})$], 129.66 [s, $C(Pz^{Me2,4Cl})$], 127.60 (d, J_{P-C} = 10 Hz, PPh_3), 133.6 (d, J_{PC} = 12 Hz, PPh). − IR (KBr): $\tilde{\nu}$ = 2477 [ν(BH)], 1988 cm^{-1} [ν(CO)].

[Tp^{Me2,4Cl}Rh(CO){P(OMe)$_3$}] (14): Complex **14** was prepared by adding $P(OMe)_3$ (0.077 mL, 0.03 mmol) to a solution of [Tp^{Me2,4Cl}Rh(CO)$_2$] (0.15 g, 0.27 mmol) in CH_2Cl_2 (20 mL). The reaction was complete within 1 h (IR monitoring). The solvent was then evaporated to leave a yellow powder, which was washed three times with hexane at 0 °C and dried in vacuo to yield 0.16 g of **14**. − ^{1}H NMR (C_6D_6, 25 °C): δ = 1.80 [s, 9 H, $(OCH_3)_3$], 2.05 [s, 9 H, $CH_3(Pz^{Me2,4Cl})$], 2.41 [s, 9 H, $CH_3(Pz^{Me2,4Cl})$]. − ^{31}P NMR (C_6D_6, 25 °C): δ = 142.24 (d, 1 P, $^1J_{Rh-P}$ = 262 Hz). − IR (KBr): $\tilde{\nu}$ = 2536 [ν(BH)], 1998 cm^{-1} [ν(CO)].

[Tp^{Me2,4Cl}Rh(CO){P(OPh)$_3$}] (15): Complex **15** was prepared by adding $P(OPh)_3$ (0.155 g, 0.591 mmol) to a solution of [Tp^{Me2,4Cl}Rh(CO)$_2$] (0.30 g, 0.54 mmol) in CH_2Cl_2 (30 mL). The reaction mixture was stirred for 4 h. The CH_2Cl_2 was then evaporated to leave a yellow powder, which was washed three times with hexane at 0 °C and dried in vacuo yielding 0.39 g of **15**. − ^{1}H NMR (C_6D_6, 25 °C): δ = 2.06 [s, 9 H, $CH_3(Pz^{Me2,4Cl})$], 2.37 [s, 9 H, $CH_3(Pz^{Me2,4Cl})$], 7.04 [m, 15 H, $P(OPh)_3$]. − ^{31}P NMR (C_6D_6, 25 °C): δ = 123.05 (d, 1 P, $^1J_{Rh-P}$ = 279 Hz). − IR (KBr): $\tilde{\nu}$ = 2494 [ν(BH)], 2007 cm^{-1} [ν(CO)]. − UV/Vis (pentane): λ_{max} = 345 nm

[Tp^{Me2,4Cl}Rh(CO){P(O*i*Pr)$_3$}] (16): Complex **16** was prepared by adding $P(OiPr)_3$ (0.145 mL, 0.59 mmol) to a solution of [Tp^{Me2,4Cl}Rh(CO)$_2$] (0.30 g, 0.54 mmol) in CH_2Cl_2 (30 mL). The volatiles were evaporated to leave a yellow powder, which was washed three times with hexane at 0 °C and dried in vacuo yielding 0.36 g of **16**. − ^{1}H NMR (C_6D_6, 25 °C): δ = 1.10 [d, 6 H, $OCH(CH_3)_2$, $^3J_{H-H}$ = 6 Hz], 2.09 [s, 9 H, $CH_3(Pz^{Me2,4Cl})$], 2.37 [s, 9 H, $CH_3(Pz^{Me2,4Cl})$], 4.51 [m, 1 H, $OCH(CH_3)_2$]. − ^{31}P NMR (C_6D_6, 25 °C): δ = 126.53 (d, 1 P, $^1J_{Rh-P}$ = 243 Hz). − IR (KBr): $\tilde{\nu}$ = 2469 [ν(BH)], 1996 cm^{-1} [ν(CO)].

[{κ^2-HB(Pz^{Me2})$_2$(HPz^{Me2})}Rh(CO)(PMe$_2$Ph)]$^+$[BF$_4$]$^-$ (4H$^+$): Complex **4H$^+$** was prepared by adding HBF_4 (25 μL, 54% in diethyl ether) to a solution of [Tp^{Me2}Rh(CO)(PMe$_2$Ph)] (0.10 g, 0.18 mmol) in diethyl ether (10 mL) at −78 °C. The solution was stirred for 15 min at this temperature and was then allowed to slowly warm to 25 °C, whereupon a white product precipitated. This solid was collected by filtration, washed with diethyl ether, and dried in vacuo yielding 0.08 g of **4H$^+$**. − ^{1}H NMR (C_6D_6, 25 °C): δ = 1.41 [dd, 3 H, J_{P-H} = 9, J_{Rh-H} = 1.6 Hz, (P*Me*$_2$Ph)], 1.47 (dd, 3 H, J_{P-H} = 9, J_{Rh-H} = 0.5 Hz, P*Me*$_2$Ph), 1.83, 2.02, 2.38, 2.43, 2.45, 2.48 [s, 3 H, *Me*(Pz^{Me2})], 7.50 (m, 5 H, PPh). − ^{31}P NMR (C_6D_6, 25 °C): δ = 15.86 (d, J_{Rh-P} = 151 Hz). − IR (KBr): $\tilde{\nu}$ = 2502 [ν(BH)], 1987 cm^{-1} [ν(CO)].

X-ray Crystal Structure Determinations: For compound **5**, data were collected at room temperature with a STOE IPDS diffractometer equipped with a graphite-oriented monochromator using Mo-K_α radiation (λ = 0.71073 Å). The final unit cell parameters were obtained by the least-squares refinement of 5000 reflections. An Enraf-Nonius CAD4F diffractometer was used for the data collection of compound **8**. For both compounds, only statistical fluctuations were observed in the intensities of standard reflections monitored throughout the course of the data collections. The structures were solved by direct methods (SIR-97)[22] and refined by least-squares methods on *F*. All H atoms attached to carbon were introduced in calculated positions [*d*(CH) = 0.96 Å] and their atomic coordinates were recalculated after each cycle. They were given isotropic thermal parameters 20% higher than those of the carbon to which they were attached. H atoms attached to boron were located by difference Fourier syntheses and their atomic and isotropic thermal parameters were refined. The absolute configuration of **5** was determined by careful examination of the sensitive reflections and refinement of Flack's enantiopole parameter.[23] Least-squares refinements were carried out by minimizing the function $\Sigma w(|F_o| - |F_c|)$, where F_o and F_c are the observed and calculated structure factors. The weighting scheme used in the final refinement cycles was $w = w'[1 - \{\Delta F/6\sigma(F_o)\}^2]^2$; here, $w' = 1/\Sigma \cong_1^n A_r T_r(x)$ with three coefficients A_r for the Chebyshev polynomial $A_r T_r(x)$, where $x = F_c/F_c(\max)$.[24] Models reached convergence with $R = \Sigma(||F_o| - |F_c||)/\Sigma(|F_o|)$ and $R_w = [\Sigma w(|F_o| - |F_c|)^2/\Sigma w(F_o)^2]^{1/2}$, giving the values listed in Table 4. The calculations were carried out with the CRYSTALS program package[25] run on a PC. Graphical representations were generated using ORTEP.[26] Crystallographic data (excluding structure factors) for the structures reported in this paper have been deposited with the Cambridge Crystallographic Data Centre as supplementary publication nos. CCDC-149636 (**5**) and -149637 (**8**). Copies of the data can be obtained free of charge on application to the CCDC, 12 Union Road, Cambridge CB2 1EZ, U.K. [Fax: (internat.) + 44-1223/336-033; E-mail: deposit@ccdc.cam.ac.uk].

Table 4. Crystal data

	5	**8**
empirical formula	$C_{29}H_{35}BN_6OPRhCH_2Cl_2$	$C_{34}H_{37}BN_6O_4PRh$
formula mass	713.26	738.40
crystal system	orthorhombic	triclinic
space group	$P2_1ca$	$P\bar{1}$
a, Å	14.222(3)	10.673(1)
b, Å	14.673(2)	12.239(2)
c, Å	15.991(7)	13.805(2)
α, °	90.0	87.43(1)
β, °	90.0	87.44(1)
γ, °	90.0	77.57(1)
V, Å^3	3337(2)	1758.1(4)
Z	4	2
ρ (calcd.) g·cm^{-3}	1.420	1.395
2θ range, °	$3 < 2\theta < 50$	$2.9 < 2\theta < 48.4$
no. of reflns. collected	6134	13956
no. of unique reflns. (R_{int})	5868 (0.020)	5189 (0.038)
reflections used	4659 [$I > 2\sigma(I)$]	4152 [$I > 2\sigma(I)$]
R, R_w	0.0271, 0.0319	0.0355, 0.0423
GoF	1.043	1.064
Flack's parameter	0.01(2)	
Variable parameters	385	429

Acknowledgments

We thank the group Electrochimie de la Direction des Etudes et Recherches of Electricité de France for financial support of part of this study and for a fellowship to V. C. We gratefully acknowledge Engelhardt-Comptoir-Lyon-Alemand-Louyot for a loan of rhodium. G. Commenges, F. Lacassin, and Y. Coppel are thanked for carrying out NMR experiments with the 400-MHz NMR spectrometer.

[1] S. Trofimenko, *J. Am. Chem. Soc.* **1966**, *88*, 1842.
[2] S. Trofimenko, *Chem. Rev.* **1993**, *93*, 943.
[3] C. Gemel, R. John, C. Slugovc, K. Mereiter, R. Schmid, K. Kirchner, *J. Chem. Soc., Dalton Trans.* **2000**, *15*, 2607.
[4] F. Malbosc, Ph. Kalck, J.-C. Daran, M. Etienne, *J. Chem. Soc., Dalton Trans.* **1999**, 271.
[5] M. Paneque, S. Sirol, M. Trujillo, E. Gutiérnez-Publa, M. Angeles Monge, E. Carmona, *Angew. Chem. Int. Ed.* **2000**, *39*, 218.
[6] U. E. Bucher, A. Currao, R. Nesper, H. Rügger, L. M. Venanzi, E. Younger, *Inorg. Chem.* **1995**, *34*, 66.
[7] M. Akita, K. Ohta, Y. Takahashi, S. Hikichi, Y. Moro-oka, *Organometallics* **1997**, *16*, 4121.
[8] C. K. Ghosh, W. A. G. Graham, *J. Am. Chem. Soc.* **1987**, *109*, 4726.
[9] A. A. Purwoko, A. J. Lees, *Inorg. Chem.* **1996**, *35*, 675.
[10] S. E. Bronsberg, H. Yang, M. C. Asplund, T. Lian, B. K. McNamara, K. T. Kotz, J. S. Yeston, M. Wilkens, H. Frei, R. G. Bergman, C. B. Harris, *Science* **1997**, *278*, 260.
[11] V. Chauby, C. Serra-Le Berre, Ph. Kalck, J.-C. Daran, G. Commenges, *Inorg. Chem.* **1996**, *35*, 6354.
[12] N. G. Connelly, D. J. H. Emslie, B. Metz, A. G. Orpen, M. J. Quayle, *Chem. Commun.* **1996**, 2289.
[13] C. K. Ghosh, Ph.D. Dissertation, University of Alberta, Canada, **1988**. In the absence of an X-ray crystal structure of **4** and of an analysis of the ν_{BH} bands, Ghosh proposed that the exchange phenomenon occurs between two isomeric trigonal bipyramids having a plane of symmetry.
[14] T. T. Derencsényi, *Inorg. Chem.* **1981**, *20*, 665.
[15] R. G. Bull, C. K. Ghosh, J. K. Hoyano, A. D. MacMaster, W. A. G. Graham, *Chem. Commun.* **1989**, 341.
[16] W. D. Jones, *Activation of Unreactive Bonds and Organic Synthesis*, Springer, Berlin, **1999**, vol. 3, p. 9−46.
[17] E. Gutiévrez, S. A. Hudson, A. Monge, E. Carmona, *J. Chem. Soc., Dalton. Trans.* **1992**, 2651.
[18] D. D. Perrin, W. L. F. Armarego, D. R. Perrin, *Purification of Laboratory Chemicals*, Pergamon Press, Oxford, **1980**.
[19] K. v. Auvers, K. Bäht, *J. Prakt. Chem.* **1927**, *116*, 65.
[20] F. J. Lalor, T. J. Desmond, G. M. Cotter, C. A. Shanahan, G. Ferguson, M. Pervez, B. Ruhl, *J. Chem. Soc., Dalton. Trans.* **1995**, 1709.
[21] S. Trofimenko, *J. Am. Chem. Soc.* **1967**, *89*, 3170.
[22] A. Altomare, M. C. Burla, M. Camalli, G. L. Cascarano, C. Giacovazzo, A. Guagliardi, A. G. G. Moliterni, G. Polidori, R. Spagni, *J. Appl. Crystallogr.* **1999**, *32*, 115−119.
[23] [23a] H. D. Flack, *Acta Crystallogr., Sect. A* **1983**, *39*, 876−881. − [23b] G. Bernardinelli, H. D. Flack, *Acta Crystallogr., Sect. A* **1985**, *41*, 500−511.
[24] E. Prince, *Mathematical Techniques in Crystallography*, Springer-Verlag, Berlin, **1982**.
[25] D. J. Watkin, C. K. Prout, J. R. Carruthers, P. W. Betteridge, *CRYSTALS Issue 11*, Chemical Crystallography Laboratory, University of Oxford, Oxford, **1999**.
[26] M. N. Burnett, C. K. Johnson, *ORTEP III, Report ORNL-6895*, Oak Ridge National Laboratory, Oak Ridge, Tennessee, **1996**.

Received December 11, 2000
[I00468]